

## The high Energy density of $\text{Pb}(\text{Zr}_{1-x}\text{Ti}_x)\text{O}_3\text{-Pb}(\text{Ni}_{1/3}\text{Nb}_{2/3})\text{O}_3$ ceramics for piezoelectric energy harvesting devices

In-Tae Seo<sup>a</sup>, Chang-Hoi Choi<sup>a</sup>, In-Young Kang<sup>a</sup>, Sahn Nahm<sup>a</sup>, Se Bin Kim<sup>b</sup>, Daniel Song<sup>b</sup>, Ju Lee<sup>b</sup>,  
Tae Hyun Sung<sup>b,\*</sup> and Jong-Hoo Paik<sup>c</sup>

<sup>a</sup>Department of Materials Science and Engineering, Korea University, 1-5 Ka, Anam-Dong, Sungbuk-Ku, Seoul 136-701, Korea

<sup>b</sup>Departments of Electric Engineering, Hanyang University, Seoul 133-791 Korea

<sup>c</sup>Korea Institute of Ceramic Engineering and Technology, Seoul 153-801, Korea

The energy density of  $0.65\text{Pb}(\text{Zr}_{1-x}\text{Ti}_x)\text{-}0.35\text{Pb}(\text{Ni}_{1/3}\text{Nb}_{2/3})\text{O}_3$  [ $0.65\text{P}(\text{Z}_{1-x}\text{T}_x)\text{-}0.35\text{PNN}$ ] ceramics has been investigated with respect to their structural variations. The  $0.65\text{P}(\text{Z}_{1-x}\text{T}_x)\text{-}0.35\text{PNN}$  ceramic with  $x = 0.58$  exhibited a morphotropic phase boundary (MPB), in which pseudo-cubic and tetragonal structures coexisted. The  $\varepsilon_{33}^T/\varepsilon_0$  value of the  $0.65\text{P}(\text{Z}_{1-x}\text{T}_x)\text{-}0.35\text{PNN}$  ceramic decreased considerably on the pseudo-cubic side of the MPB composition, while the  $d_{33}$  slowly decreased on both sides of the MPB. Because the  $g_{33}$  is given by  $d_{33}/\varepsilon_{33}^T$ , the maximum transduction coefficient ( $d_{33} \times g_{33}$ ) was obtained from the composition on the pseudo-cubic side of the MPB. In particular, the  $0.65\text{P}(\text{Z}_{0.45}\text{T}_{0.55})\text{-}0.35\text{PNN}$  ( $0.65\text{PZT55-}0.35\text{PNN}$ ) ceramic with a pseudo-cubic structure showed the maximum  $d_{33} \times g_{33}$  value of  $16,500 \times 10^{-15} \text{ m}^2/\text{N}$ . Moreover, the  $0.65\text{PZT55-}0.35\text{PNN}$  ceramics with 1.5 mol% CuO added were well sintered even at  $950^\circ\text{C}$ , and also exhibited a high  $d_{33} \times g_{33}$  value of  $15,853 \times 10^{-15} \text{ m}^2/\text{N}$ , indicating that the  $0.65\text{PZT55-}0.35\text{PNN}$  ceramic with CuO added is a good candidate material for multilayer energy harvesting devices.

**Key words:** Piezoelectric, Energy harvesting, Sintering, Dielectric constant, Ferroelectric.

### Introduction

There has been increasing interest in energy harvesting from the various wasted energies in the environment, including solar energy, thermal energy, and vibrational energy. Among these, the energy harvesting from an ambient vibrational source using piezoelectric ceramics has attracted much attention because of its high power density and potential use as a power source for wireless devices and components [1-6].

In order to use piezoelectric ceramics as energy harvesting devices, they should have a high energy density, which can be expressed by the following equation [6]:

$$u = 1/2(d \times g) (F/A)^2 \quad (1)$$

where  $d$  is the piezoelectric strain constant,  $g$  is the piezoelectric voltage constant,  $F$  is the applied force, and  $A$  is the area. According to equation (1), a high energy density can be obtained from piezoelectric materials with a large transduction coefficient ( $d \times g$ ) and many studies have been conducted to find such piezoelectric materials [7, 8]. Moreover, because  $g$  is given by  $d/e^T$ , where  $e^T$  is the dielectric constant under

constant stress conditions, a large  $d \times g$  value, and eventually a high energy density, can be obtained from piezoelectric materials with a large  $d$  value and small  $e^T$ . Many investigations have been conducted to obtain piezoelectric ceramics with, a high  $d_{33}$  value and small  $e^{T-10}$ , and piezoelectric ceramics with a composition corresponding to the rhombohedral or pseudo-cubic side of the MPB have been found to exhibit a high  $d \times g$  because of their high  $d_{33}$  but small  $e^T$  values [9, 10].

However, even though energy harvesting devices using piezoelectric ceramics generate a high power density, they produce a large voltage (~ several tens to hundreds of volts) and a small current (~ microamp scale). On the other hand, a large current is required to reduce the storage time for the storage device of a sensor node. Moreover, because the voltage capacity of a normal battery is low (about 3.0 V), there is no need for the high voltage, that is generally produced by the piezoelectric materials. Therefore, it is necessary to reduce the voltage but increase the current for piezoelectric energy harvesting device applications. An energy harvesting device with a multilayer structure can increase the current but reduce the voltage without decreasing the energy density of the piezoelectric materials.<sup>11)</sup> Therefore, it is necessary to develop energy harvesting devices with multilayer structures to reduce the voltage but increase the current. Silver metal, which is cheap and has a good conductivity, has generally been used for the electrode of such a multilayer device.

\*Corresponding author:  
Tel : +82-2-2220-4317  
Fax: +82-2-2220-2317  
E-mail: sungth@hanyang.ac.kr

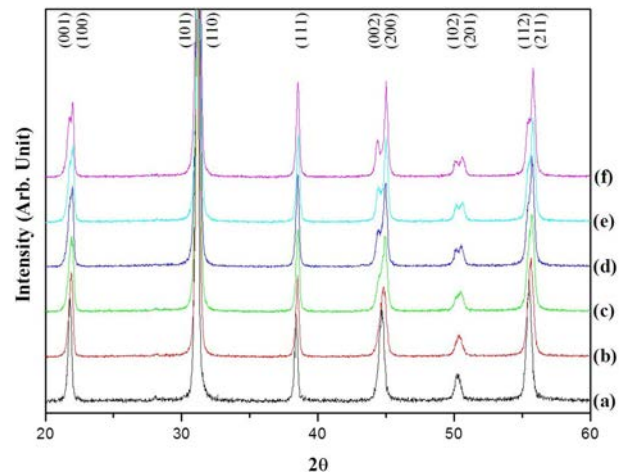
However, because the melting temperature of an Ag electrode is 961 °C, it is necessary to reduce the sintering temperature of the piezoelectric ceramics below 960 °C. The aim of this study was to find piezoelectric ceramics with high  $d_{33} \times g_{33}$  values that could be sintered below 960 °C. The  $0.65\text{Pb}(\text{Zr}_{1-x}\text{Ti}_x)\text{O}_3-0.35\text{Pb}(\text{Ni}_{1/3}\text{Nb}_{2/3})\text{O}_3$  [ $0.65\text{P}(\text{Z}_{1-x}\text{T}_x)-0.35\text{PNN}$ ] ceramics were selected for this purpose, because they are known to have high  $d_{33}$  values [12-16] and have been reported to be sintered at low temperatures [16-21].

### Experimental Procedures

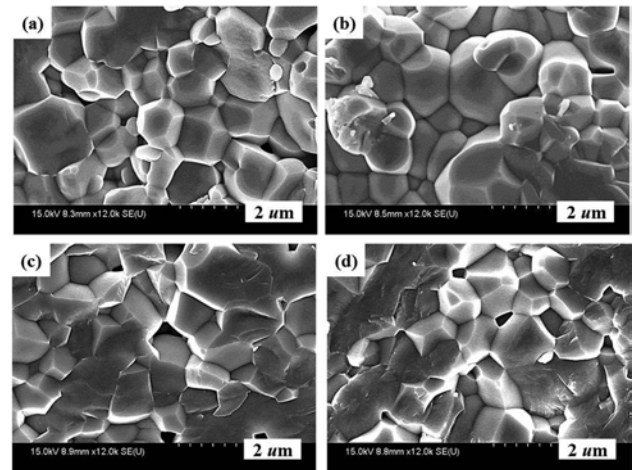
$0.65\text{P}(\text{Z}_{1-x}\text{T}_x)-0.35\text{PNN}$  ceramics with  $0.53 \leq x \leq 0.63$  were prepared from oxides with a purity of >99% by conventional solid-state synthesis. The oxide compounds,  $\text{PbO}$ ,  $\text{ZrO}_2$ ,  $\text{TiO}_2$ ,  $\text{NiO}$ , and  $\text{Nb}_2\text{O}_5$  (all from High Purity Chemicals, >99%, Japan), were mixed for 24 h in a nylon jar with zirconia balls and then dried. The dried powders were calcined at 880 °C for 4 h. After re-milling, the powders were dried, pressed into discs under a pressure of 100 kgf/cm<sup>2</sup> (9.8 MPa), and sintered at 1200 °C for 4 h. For the low temperature sintering, the calcined powders were re-milled with a CuO (High Purity Chemicals, >99%, Japan) additive. They were then dried, pressed into discs under a pressure of 100 kgf/cm<sup>2</sup>, and sintered at 950 °C for 4 h. The structural properties of the specimens were examined using X-ray diffraction (XRD: Rigaku D/max-RC, Tokyo, Japan). The densities of the sintered specimens were measured by a water-immersion method using the Archimedes-principle. A silver electrode was printed on the lapped surfaces and the specimens were polled in silicone oil at 120 °C by applying a DC field of 4.0 kV/mm for 30 minutes. The piezoelectric and dielectric properties, and the  $k_p$  value, were determined using a  $d_{33}$  meter (Micro-Epsilon Channel Product DT-3300, Raleigh, NC) and an impedance analyzer (Agilent Technologies HP 4294A, Santa Clara, CA) on the basis of the IEEE standards.

### Results and Discussion

Figures 1(a - f) show the XRD patterns of the  $0.65\text{P}(\text{Z}_{1-x}\text{T}_x)-0.35\text{PNN}$  ceramics with  $0.53 \leq x \leq 0.63$  sintered at 1200 °C for 4 h. All of the specimens had a homogeneous perovskite structure without a second phase. The specimen with  $x = 0.53$  showed the pseudo-cubic structure, and this structure was maintained until  $x = 0.57$ . When  $x$  exceeded 0.57, the tetragonal phase, which was unidentified by the separation of the peak at around 45 degrees, started to be developed. The tetragonality of the specimen increased with increasing Ti content, and a homogeneous tetragonal structures was found for the specimens with  $x \geq 0.61$ . Moreover, the MPB composition, in which the tetragonal and pseudo-cubic structure coexisted, was considered to be  $x = 0.58$ .



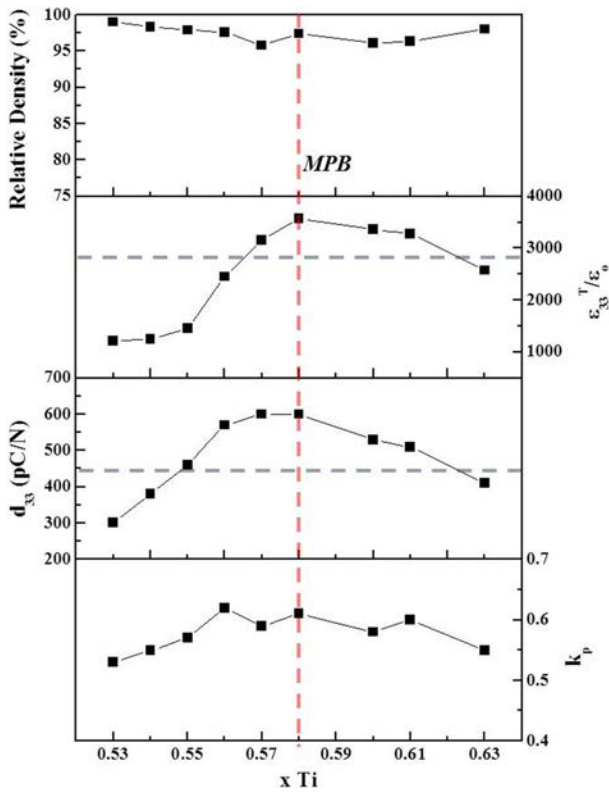
**Fig. 1.** XRD patterns of  $0.65\text{P}(\text{Z}_{1-x}\text{T}_x)-0.35\text{PNN}$  ceramics with  $0.53 \leq x \leq 0.63$  sintered at 1200 °C for 4 h: (a)  $x = 0.53$ , (b)  $x = 0.57$  (c)  $x = 0.58$ , (d)  $x = 0.6$  (e)  $x = 0.61$  and (f)  $x = 0.63$ .



**Fig. 2.** SEM images of the fractured surfaces of  $0.65\text{P}(\text{Z}_{1-x}\text{T}_x)-0.35\text{PNN}$  ceramics with  $0.55 \leq x \leq 0.61$  sintered at 1200 °C for 4 h: (a)  $x = 0.53$ , (b)  $x = 0.55$  (c)  $x = 0.58$ , and (d)  $x = 0.61$ .

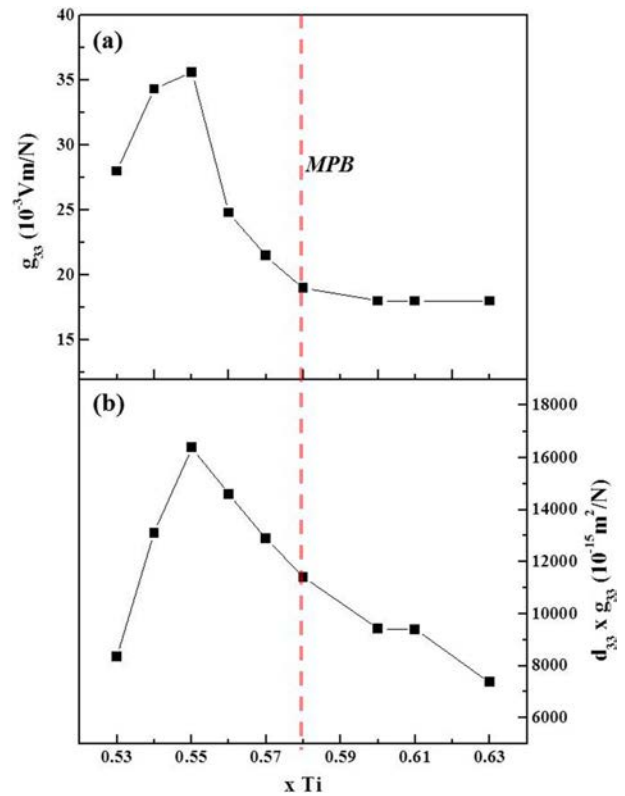
According to a previous study, the  $\epsilon_{33}^T/\epsilon_0$  value decreased with a decrease in the grain size, resulting in increased  $g_{33}$  and  $d_{33} \times g_{33}$  values. Moreover, Islam and Priya suggested that the materials constant,  $n$ , decreased with a decrease in the grain size of the ceramic, which leads to increased  $g_{33}$  and  $d_{33} \times g_{33}$  values [7, 8]. Therefore, the microstructure of the  $0.65\text{P}(\text{Z}_{1-x}\text{T}_x)-0.35\text{PNN}$  ceramics with  $0.53 \leq x \leq 0.61$  sintered at 1200 °C for 4 h, was investigated using SEM, as shown in Figures. 2(a - d). The average grain size of the specimen with the MPB composition ( $x = 0.58$ ) was approximately 2.0  $\mu\text{m}$ , and it did not change along both sides of the MPB composition. Therefore, the effect of the microstructure, including the grain size, on the  $g_{33}$  and  $d_{33} \times g_{33}$  values was not considered to be significant for the  $0.65\text{P}(\text{Z}_{1-x}\text{T}_x)-0.35\text{PNN}$  ceramics with  $0.53 \times 0.63$ , sintered at 1200 °C for 4.0 h.

Figure 3 shows the relative density,  $\epsilon_{33}^T/\epsilon_0$ ,  $d_{33}$  and  $k_p$



**Fig. 3.** Relative density,  $\epsilon_{33}^T/\epsilon_0$ ,  $d_{33}$ , and  $k_p$  values of  $0.65P(Z_{1-x}T_x)$ - $0.35PNN$  ceramics with  $0.53 \leq x \leq 0.63$  sintered at  $1200^\circ\text{C}$  for 4 h.

values of the  $0.65P(Z_{1-x}T_x)$ - $0.35PNN$  ceramics with  $0.53 \leq x \leq 0.63$  sintered at  $1200^\circ\text{C}$  for 4 h. The specimen with  $x = 0.53$  exhibited a high relative density equal to 98% of the theoretical density, which decreased only slightly with increasing Ti content. In addition, all of the specimens showed a high relative density equal to more than 96.0% of the theoretical density. The  $\epsilon_{33}^T/\epsilon_0$  value of the specimen with the MPB composition ( $x = 0.58$ ) was high (about 3560), but it decreased considerably (to 1460) for the specimen with  $x = 0.55$ , which had the pseudo-cubic structure. On the other hand, the  $\epsilon_{33}^T/\epsilon_0$  value slightly decreased to 3276 for the specimen with  $x = 0.61$ , which had the tetragonal structure. Therefore, the  $\epsilon_{33}^T/\epsilon_0$  value slowly decreased along the tetragonal side but considerably decreased along the pseudo-cubic side when the composition deviated from the MPB composition. The  $d_{33}$  value of the MPB composition was high (approximately 600 pC/N). However, it decreased when the composition deviated from the MPB composition, and the decreasing rates along both the tetragonal and pseudo-cubic sides were similar to each other. Therefore, the decreasing behavior of the  $d_{33}$  value along the pseudo-cubic side of MPB was different from that of  $\epsilon_{33}^T/\epsilon_0$ , and a high  $d_{33} \times g_{33}$  value was expected in the specimen with a pseudo-cubic composition because of this difference. The  $k_p$  value was high for the specimen with a MPB composition, and it decreased slightly, with similar decreasing rates along both sides of the MPB composition.



**Fig. 4.** Variations of the (a)  $g_{33}$  and (b)  $d_{33} \times g_{33}$  values of  $0.65P(Z_{1-x}T_x)$ - $0.35PNN$  ceramics with  $0.53 \leq x \leq 0.63$  sintered at  $1200^\circ\text{C}$  for 4 h.

Variations of the  $g_{33}$  and  $d_{33} \times g_{33}$  values are illustrated in Figures 4(a) and (b), respectively. The  $g_{33}$  value of the specimen with an MPB composition ( $x = 0.58$ ) was low ( $19.0 \times 10^{-3} \text{Vm/N}$ ) because of the large  $\epsilon_{33}^T/\epsilon_0$  value. Moreover, the  $g_{33}$  values decreased with increasing Ti content, and all of the specimens with a tetragonal structure exhibited a low  $g_{33}$  value of less than  $19.0 \times 10^{-3} \text{Vm/N}$ . On the other hand, the  $g_{33}$  value increased when the composition deviated from the MPB composition to the pseudo-cubic side (decreasing Ti content), and a maximum  $g_{33}$  value of  $35.6 \times 10^{-3} \text{Vm/N}$  was obtained from the specimen with  $x = 0.55$ . The increase in the  $g_{33}$  value was related to the decreased  $\epsilon_{33}^T/\epsilon_0$ , while a high  $d_{33}$  value was maintained. The  $g_{33}$  value decreased when  $x$  was smaller than 0.55, probably because of the decrease in the  $d_{33}$  value. The  $d_{33} \times g_{33}$  value is shown in Figure 4(b). The specimen with an MPB composition exhibited a small  $d_{33} \times g_{33}$  value of  $11,410 \times 10^{-15} \text{m}^2/\text{N}$ , which decreased along the tetragonal side of the MPB composition. However, the  $d_{33} \times g_{33}$  value increased along the pseudo-cubic side of the MPB composition, and a maximum  $d_{33} \times g_{33}$  value of  $16,500 \times 10^{-15} \text{m}^2/\text{N}$  was obtained from the specimen with  $x = 0.55$ . The high  $d_{33} \times g_{33}$  value was a result of the difference in the decreasing behaviors of the  $\epsilon_{33}^T/\epsilon_0$  and  $d_{33}$  values along the pseudo-cubic side of the MPB composition.

CuO was added to the  $0.65P(Z_{0.45}T_{0.55})$ - $0.35PNN$  ( $0.65PZT55$ - $0.35PNN$ ) ceramics, which showed the

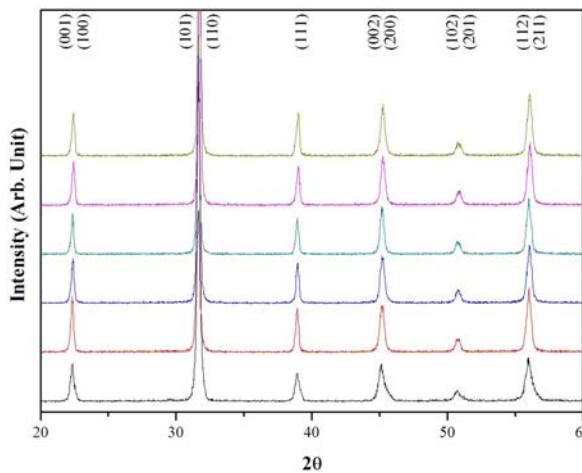


**Fig. 5.** XRD patterns of 0.65PZT55-0.35PNN +  $y$  mol% CuO ceramics with  $0.0 \leq y \leq 3.0$  sintered at 950 °C for 4 h: (a)  $y = 0.0$ , (b)  $y = 0.5$ , (c)  $y = 1.0$ , (d)  $y = 1.5$ , (e)  $y = 2.0$  and (f)  $y = 3.0$ .

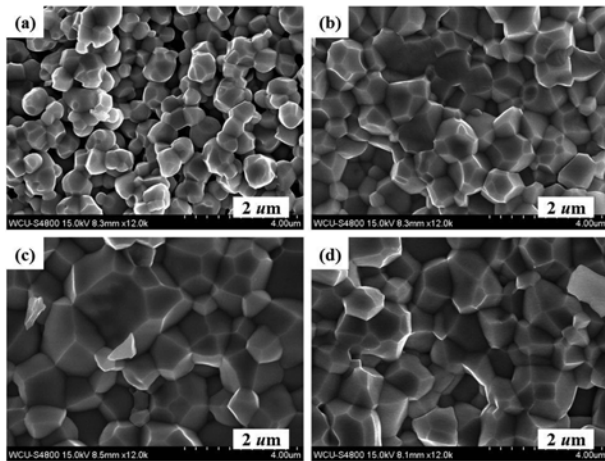


**Fig. 6.** SEM images of the fracture surfaces of 0.65PZT55-0.35PNN +  $y$  mol% CuO ceramics with  $0.0 \leq y \leq 3.0$  sintered at 950 °C for 4 h: (a)  $y = 0.0$ , (b)  $y = 1.0$ , (c)  $y = 1.5$  and (d)  $y = 3.0$ .

maximum  $g_{33}$  and  $d_{33} \times g_{33}$  values, to reduce their sintering temperature for application to a multilayer energy harvester. Figure 5 shows the XRD patterns of the 0.65PZT55-0.35PNN +  $y$  mol% CuO ceramics with  $0.0 \leq y \leq 3.0$  sintered at 950 °C for 4 h. A homogeneous 0.65PZT55-0.35PNN phase developed without the CuO or CuO-related phase. Figures 6(a - d) show the SEM images of the fractured surfaces of the 0.65PZT55-0.35PNN +  $y$  mol% CuO ceramics with  $0.0 \leq y \leq 3.0$  sintered at 950 °C for 4 h. For the specimen with  $y = 0$ , a porous microstructure was developed, as shown in Figure 6(a), but a dense microstructure formed when the amount of CuO exceeded 0.5 mol% (see Figures. 6(b - d)). CuO has been reported to react with PbO and form a liquid phase, which assisted the densification of the specimen at low temperature.<sup>22</sup> Therefore, even though the CuO related second phase was not observed, the CuO was considered to be used to form the liquid phase. The average grain size of these specimens was approximately 2.0  $\mu\text{m}$ , which was

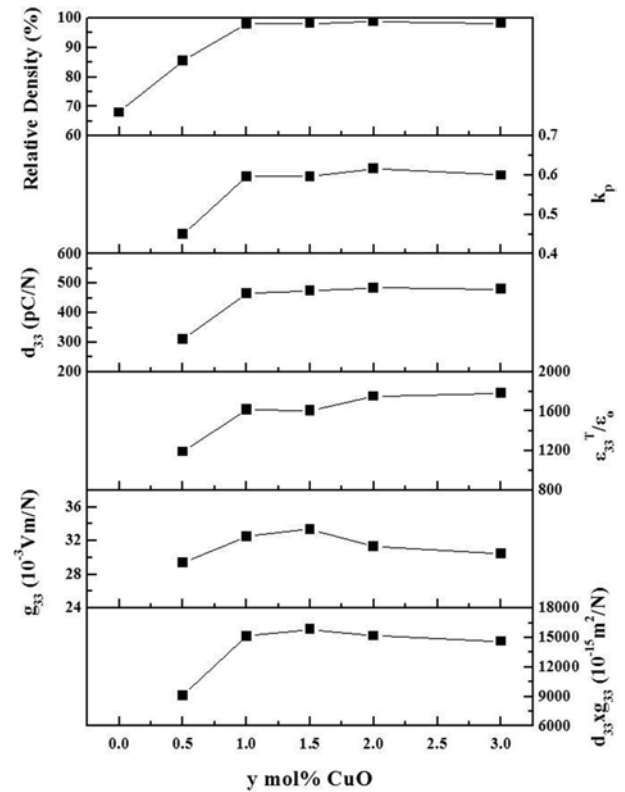


**Fig. 7.** Relative density,  $k_p$ ,  $\epsilon_{33}^T/\epsilon_0$ ,  $d_{33}$ ,  $g_{33}$  and  $d_{33} \times g_{33}$  values of 0.65PZT55-0.35PNN +  $y$  mol% CuO ceramics with  $0.0 \leq y \leq 3.0$  sintered at 950 °C for 4 h.

similar to that of the 0.65PZT55-0.35PNN ceramic sintered at 1200 °C. Therefore, the influence of the grain size on the  $\epsilon_{33}^T/\epsilon_0$  value, and eventually the  $g_{33}$  and  $d_{33} \times g_{33}$  values, is expected to be small.

Figure 7 shows the relative density,  $k_p$ ,  $\epsilon_{33}^T/\epsilon_0$ ,  $d_{33}$ ,  $g_{33}$ , and  $d_{33} \times g_{33}$  values of the 0.65PZT55-0.35PNN +  $y$  mol% CuO ceramics with  $0.0 \leq y \leq 3.0$  sintered at 950 °C for 4 h. The relative density of the specimen with  $y = 0.0$ , was very low but increased as the CuO content increased to a saturated value equal to 98% of the theoretical density for the specimen with  $y = 1.0$ . The  $k_p$  value of the 0.65PZT55-0.35PNN ceramic could not be measured because of the low density. However, it increased with the addition of a small amount of CuO, and a saturated value of 0.6 was obtained for the specimen with  $y = 1.0$ . The variations in the  $\epsilon_{33}^T/\epsilon_0$  and  $d_{33}$  values with respect to CuO were similar to that of the  $k_p$  value, indicating that the  $\epsilon_{33}^T/\epsilon_0$  and  $d_{33}$  values are considerably affected by the relative density. The  $g_{33}$  and  $d_{33} \times g_{33}$  values are also illustrated in Figure. 7. Although these were immeasurable for the specimen with  $x = 0.0$  because of the low density, they increased with the addition of CuO. Maximum  $g_{33}$  and  $d_{33} \times g_{33}$  values of  $33 \times 10^{-3} \text{Vm/N}$  and  $15,853 \times 10^{-15} \text{m}^2/\text{N}$ , respectively, were obtained from the specimen with  $y = 1.5$ . These values were slightly lower than the  $g_{33}$  and  $d_{33} \times g_{33}$  values obtained from the 0.65PZT55-0.35PNN ceramic sintered at 1200 °C but are still high

for specimens sintered at a low temperature of 950 °C. Therefore, the CuO-added 0.65PZT55-0.35PNN ceramic could a good candidate material for a multilayer energy harvesting device.

### Conclusions

The 0.65P( $Z_{1-x}T_x$ )-0.35PNN ceramic with  $x = 0.53$  had a pseudo-cubic structure and this structure was maintained until  $x = 0.57$ . When  $x$  exceeded 0.57, a tetragonal phase started to be developed, and a homogeneous tetragonal structure was found for the specimens with  $x \geq 0.61$ . Moreover, the MPB composition, in which the tetragonal and pseudo-cubic structure coexisted, was considered to be  $x = 0.58$ . The average grain size for all of the specimens was about 2.0  $\mu\text{m}$ . For these specimens, the decreasing behavior of  $\epsilon_{33}^T/\epsilon_0$  was different from that of the  $d_{33}$  value on the pseudo-cubic side of the MPB composition and this difference significantly influenced the  $g_{33}$  and  $d_{33} \times g_{33}$  values. The maximum  $g_{33}$  and  $d_{33} \times g_{33}$  values were found for the specimen whose composition was on the pseudo-cubic side of the MPB composition. In particular, the highest  $d_{33} \times g_{33}$  value of  $16,500 \times 10^{-15} \text{ m}^2/\text{N}$  was obtained from the 0.65PZT55-0.35PNN specimen. CuO was added to decrease the sintering temperature of the 0.65PZT55-0.35PNN specimen and it was well sintered even at 950 °C when the CuO content exceeded 0.5 mol%. However, the variation in the grain size with the CuO content was negligible for 0.65PZT55-0.35PNN ceramics sintered at 950°C. In particular, the 1.5 mol% CuO-added specimen showed the highest  $g_{33}$  and  $d_{33} \times g_{33}$  values of  $33.3 \times 10^{-3} \text{ Vm/N}$  and  $15,853 \times 10^{-15} \text{ m}^2/\text{N}$ , respectively, even though it was sintered at 950 °C. Therefore, the CuO-added 0.65PZT55-0.35PNN ceramic could be a good candidate material for a multilayer energy harvesting device.

### Acknowledgement

This work was supported by the research fund of Hanyang University (HY-2010-n).

### References

1. S. Priya: J. Electroceram. 19 (2007) 165-182.
2. A. Erturk and D.J. Inman: Energy Harvesting Technologies, Springer, MA (2008).
3. R. Anton and H.A. Sodano: Smart Mater. Struct. 16 (2007) R1-R21.
4. A. Sodano, D.J. Inman, and G. Park: Shock Vib. Dig. 36 (2004) 197-205.
5. S. Priya, J. Ryu, C.S. Park, J. Oliver, J.J. Choi, and D.S. Park: Sensors 9 (2009) 6362-6384.
6. S. Priya: IEEE Trans. Ultrason. Ferroelectr. Freq. Control 57 (2010) 2610-2612.
7. A. Islam and S. Priya: Appl. Phys. Lett. 88 (2006) 032903-1-3.
8. A. Islam and S. Priya: J. Am. Ceram. Soc. 89 (2006) 3147-3156.
9. Y.J. Cha, I.T. Seo, I.Y. Kang, S.B. Shin, J.H. Choi, S. Nahm, T.H. Seung, and J.H. Paik: J. Appl. Phys. 110 (2011) 084111-1-6.
10. I.T. Seo, Y.J. Cha, I.Y. Kang, J.H. Choi, S. Nahm, T.H. Seung, and J.H. Paik: J. Am. Ceram. Soc. 94 (2011) 3629-3631.
11. H.C. Song, H.C. Kim, C.Y. Kang, H.J. Kim, S.J. Yoon and D.Y. Jeong: J. Electroceram. 23 (2009) 301-304.
12. H. Banno, T. Tsunooka, and I. Shimano: Proceedings 1st Meeting on Ferroelectric Materials and Application, Edited by Omoto, and Kumada, Kyoto (1997).
13. M. Kondo, M. Hida, M. Tsukada, K. Kurihara, and N. Kamehara: Ceram. Soc. Jpn. 105 (1997) 719-721.
14. D. Luff, R. Lane, K.R. Brown, and H.J. Marshall: Trans. J. Br. Ceram. Soc. 73 (1974) 251-264.
15. J.H. Moon, H.M. Jang, and B.D. You: J. Mater. Res. 8 (1993) 3184-3191.
16. C.W. Ahn, S.Y. Noh, S. Nahm, J.H. Ryu, K. Uchino, S.J. Yoon, and J.S. Song: Jpn. J. Appl. Phys. 42 (2003) 5676-5680.
17. G. Zhilun, L. Longtu, G. Suhua, and Z. Xiaowen: J. Am. Ceram. Soc. 72 (1989) 486-491.
18. K. Shiratsuyu, K. Hayashi, A. Ando, and Y. Sakabe: Jpn. J. Appl. Phys. 39 (2000) 5609-5612.
19. S.Y. Chu and C.S. Hsieh: J. Mater. Sci. Lett. 19 (2000) 609-612.
20. C.W. Ahn, S. Nahm, J.H. Ryu, K. Uchino, S.J. Yoon, S.J. Jung, and J.S. Song: Jpn. J. Appl. Phys. 43 (2003) 205-210.
21. T. Hayashi, J. Tomizawa, T. Hasegawa, and Y. Akiyama: J. Eur. Ceram. Soc. 24 (2004) 1037-1039.
22. C.H. Nam, H.Y. Park, I.T. Seo, J.H. Choi, M.R. Joung, S. Nahm, H.J. Lee, Y.H. Kim and T.H. Sung: J. Am. Ceram. Soc. 94 (2011) 3442-3448.